

## **Influence of the composition and crystalline phase of electrodeposited CoNi films in the preparation of CoNi oxidized surfaces as electrodes for urea electro-oxidation**

J. Vilana, E. Gómez, E. Vallés\*

Ge-CPN, Departament de Química Física and Institut de Nanociència i Nanotecnologia (IN<sup>2</sup>UB), Universitat de Barcelona, Martí i Franquès 1, 08028 Barcelona, Spain.

\*Author to whom correspondence should be addressed

e-mail: e.valles@ub.edu

Phone: +34 934039238

Fax: +34 934021231

---

### **Abstract:**

Oxidized species of CoNi have been obtained by means of electrodeposition of CoNi films and posterior electro-oxidation, to obtain electrodes able to be catalysts of oxidative reactions in alkaline medium. The products of electro-oxidation formed, which depend on the composition and the crystal phase of CoNi deposits, have been identified; for this, Co-fcc, Co-hcp, Co<sub>7</sub>Ni<sub>3</sub>-fcc, Co<sub>7</sub>Ni<sub>3</sub>-hcp, Co<sub>5</sub>Ni<sub>5</sub>-fcc and Ni-fcc films have been electrodeposited and oxidized. The influence of the crystalline phase of the films in the nature of the superficial oxides formed has been demonstrated: the electrodes prepared from CoNi-fcc films contained  $\gamma$ -Co<sub>x</sub>Ni<sub>(1-x)</sub>(OH)<sub>2</sub>, while those prepared from Co<sub>7</sub>Ni<sub>3</sub>-hcp films contained Co<sub>2</sub>NiO<sub>4</sub> and  $\gamma$ -Co<sub>x</sub>Ni<sub>(1-x)</sub>(OH)<sub>2</sub>. The catalytic behaviour of the electro-oxidized electrodes for urea electro-oxidation was evaluated. Separate tests were performed to differentiate the influence of the composition and the crystalline structure of the initial films and, therefore, of the different oxidized species formed. The electrodes prepared by electro-oxidation of the Co<sub>7</sub>Ni<sub>3</sub>-hcp films show better electro-catalytic performance for urea's oxidation than those obtained by oxidation of the Co<sub>7</sub>Ni<sub>3</sub>-fcc, because they induce higher intensity, lower onset potential and lesser simultaneous oxygen evolution, becoming a good anode for urea electro-oxidation in urea electrolysis for hydrogen production or waste water treatment.

**Keywords:** CoNi oxidized surfaces Electrodeposition Catalytic substrates in basic media  
Urea electro-oxidation

## 1. Introduction

Oxidized species of cobalt (Co-Ox), nickel (Ni-Ox) and cobalt-nickel (CoNi-Ox) have been extensively investigated during many years because their importance as potential electrode materials to favour several electrochemical reactions in basic media [A20][CV1][CV2][R10]. In the last decade, different authors have demonstrated the excellent performance of these compounds for some electrochemical reactions, sometimes as an alternative to noble metals, proposing them for catalysis and sensing fields [A20][A26]. The oxidized species of Co, Ni and CoNi have been proposed as sensors of biomolecules as glucose [A3] or uric acid [A5], catalysts for methanol electro-oxidation [B1] and evolution of hydrogen [A4] and oxygen [A25]. Moreover, due to their pseudocapacitive properties, they have proposed as potential materials for supercapacitors [A1][A7][A12][A17][A19][ES5][R5][R6]. Recently, the CoNi-Ox species have been also proposed as promising electrode materials for urea electro-oxidation, due to the interest of this reaction in the fields of environmental electrochemistry or hydrogen production [A6][A8][A10][A11][A18][A25].

Therefore, the easy and controllable preparation of the CoNi-Ox species to be used as electrode materials and the knowledge of the relation between the nature of these species and their performance for electrochemical reactions is fundamental to apply them as electro-catalysts. The CoNi-Ox species have been frequently directly synthesised by chemical or electrochemical methods. The interest of this work is the synthesis of different CoNi-Ox species by oxidation of easily prepared CoNi electrodeposited films, and the identification of the species obtained in each case, in order to correlate them with the electro-catalytic performance. The synthesis will be, therefore, in two steps: in the first step, the CoNi alloys are deposited and, in the second step, they are oxidized by electrochemical methods. The electrodeposition method will permit to obtain CoNi films adherent to the substrate, of different composition ( $\text{Co}_x\text{Ni}_{(1-x)}$ ) and crystalline structure, as the manner that the posterior electro-oxidation will permit to obtain different adherent CoNi-Ox species. To attain these objectives, we will focus the study in 1) preparing and identifying the CoNi-Ox species obtained by electro-oxidation of CoNi electrodeposited films, 2) obtaining different crystalline phases of the CoNi alloys, taking advantage of the developed methods by ourselves [B2][B4], to investigate if the crystalline structure of the alloy has influence on the

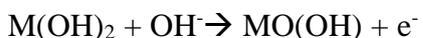
CoNi-Ox species obtained, and 3) testing of the performance of these species on the catalytic electro-oxidation of urea.

Most of the previous works about the application of CoNi-Ox species in catalysis of electrochemical reactions analyse the performance of the catalyst as a function of the Ni/(Ni+Co) ratio in the oxides-hydroxides. Now we analyse the nature of the electro-oxidised CoNi-Ox species obtained from alloys with the same ratio of metals but different crystalline phase. The crystalline phases of the electrodeposited pure metals can be: face-centered cubic for nickel (Ni-fcc) and hexagonal compact (Co-hcp) or face-centered cubic (Co-fcc) for cobalt [B5]. The CoNi alloys can only be deposited in fcc phase when atomic percentage of cobalt is lower than 60%, whereas when is higher than 60%, the alloy can be deposited in fcc, hcp or mixed phases [B4][B3][B2]. According with that, we try to prepare Co<sub>7</sub>Ni<sub>3</sub> films as Co<sub>7</sub>Ni<sub>3</sub>-hcp and Co<sub>7</sub>Ni<sub>3</sub>-fcc, which will be posteriorly electro-oxidized. From our best knowledge, no similar investigation was previously developed. In order to facilitate the interpretation of the results, films of Ni-fcc, Co-fcc, Co-hcp and Co<sub>5</sub>Ni<sub>5</sub> will be also electrodeposited for posterior electro-oxidation and characterization.

There is a general agreement that the catalytic Ni-Ox or Co-Ox species for the electro-oxidation of some molecules as glucose or methanol are the M(III) oxy-hydroxides, of general formula MO(OH), accordingly to the reaction:



being the MO(OH) species the electro-oxidized products, in basic media, of the corresponding M(II) oxides or hydroxides:



However, different structures or phases of oxides and hydroxides of these metals can be formed. Oxidized products of nickel are described in a review of David S. Hall et al [ES6], in which Ni(II) species as  $\alpha$ -Ni(OH)<sub>2</sub>,  $\beta$ -Ni(OH)<sub>2</sub> and NiO can be after electro-oxidized to form Ni(III) species as  $\beta$ -NiO(OH) or  $\gamma$ -NiO(OH). The Co-Ox species formed from cobalt electro-oxidation have been described as  $\alpha$ -Co(OH)<sub>2</sub>,  $\beta$ -Co(OH)<sub>2</sub>, Co<sub>3</sub>O<sub>4</sub> or CoO(OH) [A15][R4][ES3]. The species present on CoNi films after electro-oxidation will be, at least, of the same complexity, with mixed oxides and hydroxides. Each one of these species will present a different catalytic effect for the electrochemical oxidation of molecules. In our study we analyse the influence of the crystalline phase of the electrodeposited CoNi films of the

same composition ( $\text{Co}_7\text{Ni}_3\text{-fcc}$  and  $\text{Co}_7\text{Ni}_3\text{-hcp}$ ) in the oxidized species formed, and the influence of the composition of the films for the same crystalline phase ( $\text{Co}_7\text{Ni}_3\text{-fcc}$  and  $\text{Co}_5\text{Ni}_5\text{-fcc}$ ). The electrochemical synthesis of different types of CoNi films (phase and composition) from a single solution has been tested [B4][B2] and, if the electro-oxidation leads to different CoNi-Ox species, the electrodeposition + electro-oxidation procedure can be an easy method to obtain different CoNi-Ox species with different catalytic performance. The electrodes containing these different CoNi-Ox species will be tested for the catalytic electro-oxidation of urea, for which the catalytic effect of the NiO(OH) has been detected [A10][A11]

## 2. Experimental

All the deposits were potentiostatically prepared from deoxygenated solutions prepared using pure Millipore Milli Q water. The deposits of CoNi of different composition and crystal phase ( $\text{Co}_5\text{Ni}_5\text{-fcc}$  and  $\text{Co}_7\text{Ni}_3\text{-hcp}$ ) were obtained at 21 °C in a  $\text{CoCl}_2$  0.2 M +  $\text{NiCl}_2$  0.9 M +  $\text{H}_3\text{BO}_3$  0.5 M, pH 3, solution (“CoNi Solution”). By using the same electrolytic bath, but at 26 °C and 300 rpm,  $\text{Co}_7\text{Ni}_3\text{-fcc}$  deposits were prepared. The pure Ni-fcc deposits were obtained at 21 °C in a  $\text{NiCl}_2$  0.5 M +  $\text{H}_3\text{BO}_3$  0.5 M, pH 3, solution (“Ni Solution”). Co-hcp deposits were obtained at 21 °C in a  $\text{CoCl}_2$  0.5 M +  $\text{H}_3\text{BO}_3$  0.5 M, pH 3, solution (“Co1 Solution”), whereas the Co-fcc deposits were prepared at 21 °C in a  $\text{CoCl}_2$  0.5 M +  $\text{C}_6\text{H}_8\text{O}_7$  0.5 M solution, at pH = 1.5 adjusted with HCl (“Co2 Solution”).

The deposits were prepared on flat silicon pieces with a Ti(10 nm)/Au(100 nm) seed layer (supplied by IMB-CNM.CSIC (Centro Nacional de Microelectrónica)); the exposed area of the substrates in the solution was 0.25 cm<sup>2</sup>. A platinum spiral and an Ag/AgCl/KCl 3 M (Methrom) were used as auxiliary and reference electrodes, respectively. For the electro-oxidation of the deposits and the urea, a Luggin capillary with NaOH 0.5 M was used to contact the reference electrode with the working solution. The electrochemical experiments (deposits preparation, deposits oxidation and urea oxidation) were carried out with a Potentiostat/Galvanostat Autolab PGSTAT30, controlled with the GPES software.

The composition of the deposits was determined by an X-Ray Fluorescence (XRF) Fisherscope system XDAL with WinFTM XDAL Ver6.19 software. Both the electrodeposited materials and the corresponding oxidized species were observed by Field emission Scanning Electron Microscopy (FE-SEM) by using JSM-7100F Hitachi equipment. The thickness and

roughness of the CoNi films were analyzed by a Leica DCM 3D interferometer and LeicaMap software. Raman Microspectroscopy analysis was performed with a LabRam HR equipment with a 532nm green LED.

The electrodes for urea electro-oxidation were prepared by consecutive cyclic voltammeteries of the prepared electrodeposits (Co, Ni and CoNi) in a 0.5 M NaOH solution, in order to obtain the oxidized species. A 0.5M NaOH + 0.1M urea (of analytical grade reagents) were used for the test of urea oxidation over the oxidized deposits.

The electrodeposits prepared were also introduced in 0.5 M NaOH solution for both the corrosion test and the accumulation of oxidized species (Co-Ox, Ni-Ox, CoNi-Ox) in order to identify them by Raman. For the corrosion test, after the stabilization of the potential ( $E_{ss}$ ) in open circuit conditions, potentiodynamic curves at  $0.1 \text{ mV s}^{-1}$  were recorded from  $E_{ss}-300 \text{ mV}$  to around  $E_{ss}+400 \text{ mV}$ .

### 3. Results and discussion

#### 3.1. Synthesis and characterization of the electrodeposits

Electrodeposition of the films was performed by using the electrolytic solutions described in the Experimental section and the conditions detailed in Table 1. The charge deposited was  $Q=4 \text{ C cm}^{-2}$  in all cases. The thickness of the deposited films was around 1.5-2  $\mu\text{m}$ , depending on the morphology and grain size of each deposit. The conditions to prepare the pure metals have been selected according to the bibliography, in order to obtain the desired crystalline phase [26].

Deposit	Electrolytic solution	Temperature (°C)	E / mV	Stirring speed (rpm)
Co-fcc	Co2	21	- 800	-
Co-hcp	Co1	21	- 1000	-
Ni-fcc	Ni	21	- 1000	-
Co <sub>5</sub> Ni <sub>5</sub> -fcc	CoNi	21	- 1000	-
Co <sub>7</sub> Ni <sub>3</sub> -fcc	CoNi	26	- 800	300
Co <sub>7</sub> Ni <sub>3</sub> -hcp	CoNi	21	- 800	-

**Table 1.** *Electrolytic bath and conditions for the preparation of the metals and alloy films*

The SEM images of the different deposits prepared are shown in Figure 1. The films of pure metals present the expected morphology, according to the preparation conditions: nickel deposit show a nodular morphology characteristic of the Ni-fcc crystalline phase, whereas cobalt deposits show very different morphologies as corresponds to their different crystalline phase: fine grained deposits for the Co-fcc and acicular rough morphology characteristic of the Co-hcp deposits []. The morphology of the CoNi deposits seems already corroborate the crystalline phase desired in each case: the hcp phase for one of the  $\text{Co}_7\text{Ni}_3$  deposits (acicular rough one) and the fcc phase for the flat fine-grained  $\text{Co}_7\text{Ni}_3$  and  $\text{Co}_5\text{Ni}_5$  deposits. Really, when X-Ray diffraction was used to characterize these deposits, the crystalline phase was corroborated, as the manner that we can affirm that  $\text{Co}_5\text{Ni}_5$ -fcc,  $\text{Co}_7\text{Ni}_3$ -fcc  $\text{Co}_7\text{Ni}_3$ -hcp have been obtained (Figure 2).

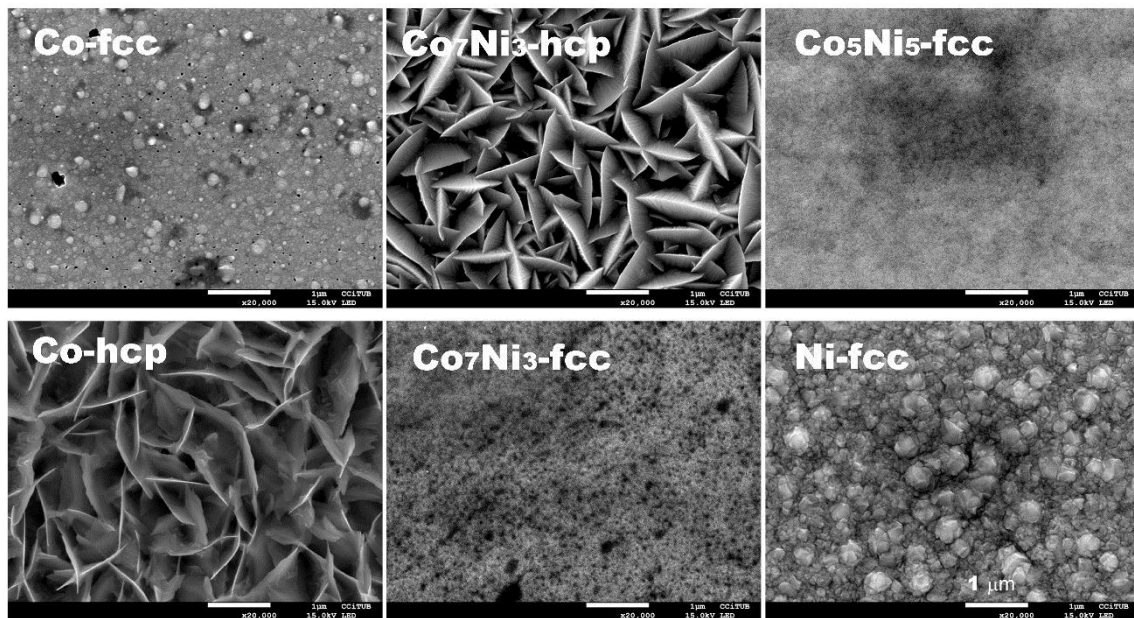


**Figure 1:** *FE-SEM images of electrodeposited metals and alloys. Scale bar: 1 μm*

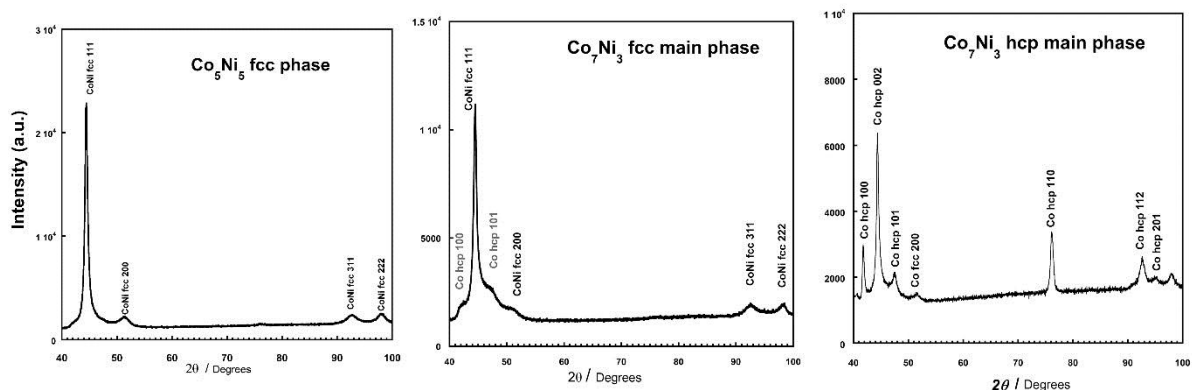


**Figure 2:** XRD of electrodeposited CoNi films of Figure 1

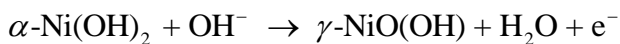
### 3.2. Electro-oxidation of the electrodeposits

The synthesised electrodeposits were introduced during 5 minutes in NaOH 0.5 M to oxidize the metals to metal (II) hydroxides. After that, and in order to induce the formation of MO(OH) species, the substrates were subjected to successive cyclic voltammetry (CV) in the same solution, in the -0.1 to 0.6 V range, achieving a constant voltammetric profile (50 cycles for Co samples and 100 cycles for Ni and CoNi samples). Figure 3 shows the evolution of the voltammetric profile from the first scan (dotted line) to the successive ones (grey lines) and the final stationary scan (black line). The voltammetry profile is in each case different and we try to interpret of the profiles of the CoNi deposits taking into account those corresponding to the pure metals and the bibliographic information.

In the case of nickel deposits, the oxidation of the Ni(OH)<sub>2</sub> to Ni(III) species has been analysed (Figure 3, Ni-fcc). In the first voltammetric scan, a non-well defined couple of peaks is detected. The stationary scan show a more clear profile where the oxidation peak has been shifted to positive potentials, appearing at around 440 mV. The main reduction current appears as a peak centred at 370 mV. There is a general agreement to assign this couple to the reaction: (doublet)



although some authors propose the existence of two forms of nickel hydroxides, which can be oxidized to two forms of nickel oxo-hydroxides[3][2][28][29]:



The  $\beta$ -Ni(OH)<sub>2</sub> is the more crystalline phase and thermodynamically more stable. The  $\alpha$ -Ni(OH)<sub>2</sub> evolves, in alkaline media, to  $\beta$ -Ni(OH)<sub>2</sub>; this change can be done by ageing or it can be observed in the cyclic voltammeteries by a shift of the anodic and cathodic peaks to more positive potentials, as described by Kim et al. [3]. This was also observed in films of NiPt by Huang et al. [30]. Therefore, we can assign the main peaks (442/370 mV) in the stationary cyclic voltammetry of the initially Ni-fcc oxidized deposit to the  $\beta$ -Ni(OH)<sub>2</sub>/ $\beta$ -NiO(OH) redox couple, whereas the reduction shoulder at 300 mV agrees with the reduction of the NiO(OH) species to  $\alpha$ -Ni(OH)<sub>2</sub>. This assignment agrees with the results of other authors [3][29][30][31], although the exact position of the peaks is depending on the OH<sup>-</sup> concentration and the nature of the alkaline cation [31].

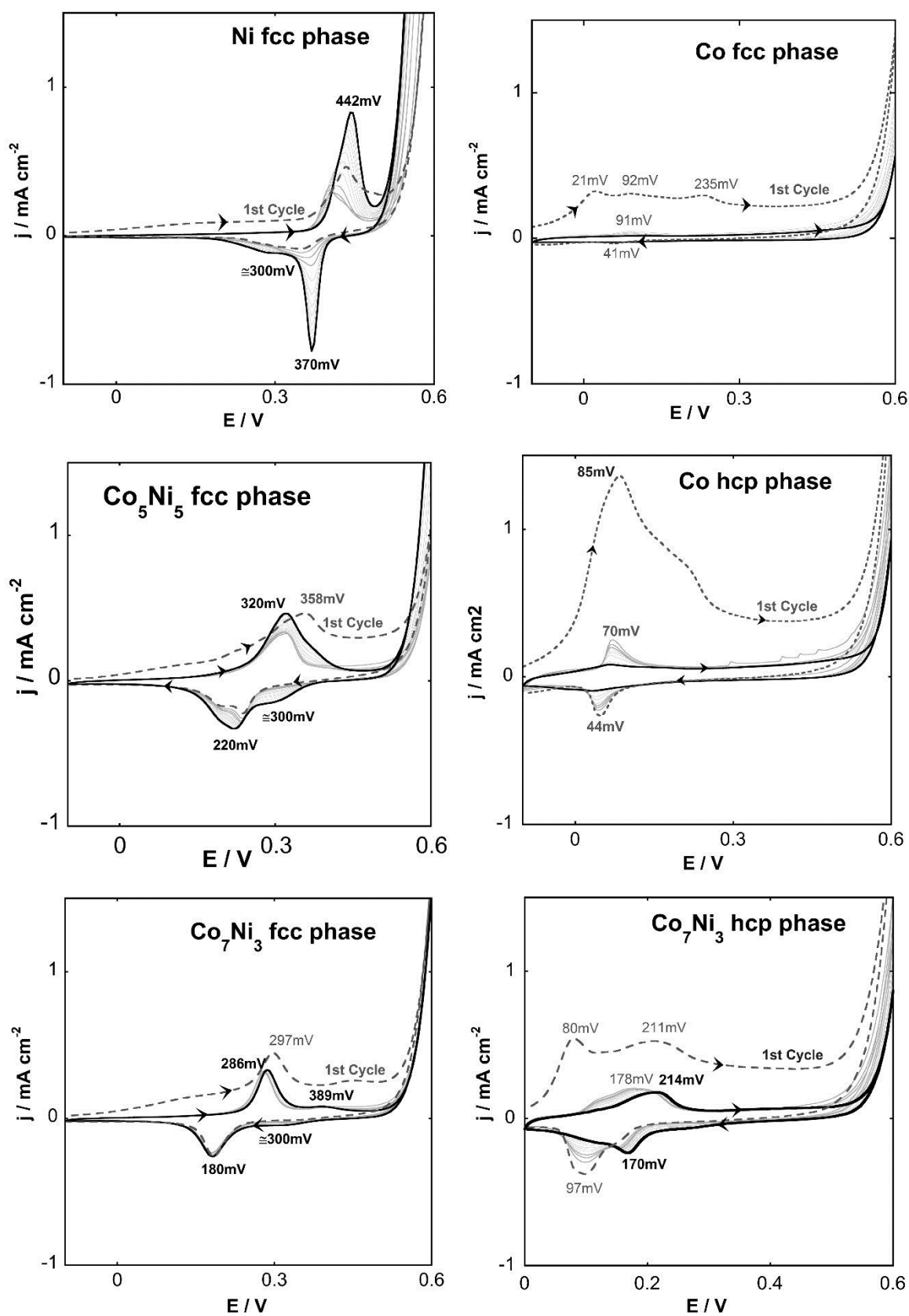


**Figure 3:** Cyclic voltammeteries in  $\text{NaOH } 0.5 \text{ M}$ , at  $50 \text{ mV s}^{-1}$ , of the electrodepositing films, after immersion during 5 minutes in  $\text{NaOH } 0.5 \text{ M}$ . ( $E$  vs  $\text{Ag/AgCl/KCl } 3\text{M}$  reference electrode)

The first scan of the Co-fcc/Co(OH)<sub>2</sub> and Co-hcp/Co(OH)<sub>2</sub> substrates show significant oxidation, especially in the case of the Co-hcp. After that, the stationary voltammetric profiles show a clear passivation of the surface, being more pronounced in the case of the Co-fcc film, for which no current is detected after a few cycles. Therefore, a passivating layer of cobalt oxide or hydroxide is formed; being the more stable compounds of Co-Ox species the cubic spinel Co<sub>3</sub>O<sub>4</sub>[28] and β-Co(OH)<sub>2</sub>[32]. Probably, the oxidation of β-Co(OH)<sub>2</sub> to Co<sub>3</sub>O<sub>4</sub> leads to a passivation of the substrate. The Co<sub>3</sub>O<sub>4</sub> oxidation to CoO(OH) is not detected in Figure 3, because the corresponding oxidation peak should appear just before of oxygen evolution, at around 500-550mV [34]. The stability of the mixed Co(II)/(III) oxide, the spinel Co<sub>3</sub>O<sub>4</sub>, doesn't favour its electro-oxidation to CoO(OH)[33]. The passivating layer is also the cause of the shifting of the oxygen evolution to more positive potentials during the cycling.

The voltammetry profiles of the oxidised CoNi films are intermediate between those of oxidized Co and Ni, although the specific voltammetric response varies as a function of the composition and crystalline phase of the alloy films. The stationary scans show anodic/cathodic peaks, but of decreasing intensity as the Co content in the deposits increases. Also, the peaks gradually shift to less positive values as the cobalt percentage increases, which agree with the results found for other authors independently of the synthesis method [35][36][9][37][21][38][14]. This demonstrates that the CoNi deposits prepared from, in NaOH solution, mixed hydroxides of Ni(II) and Co(II), instead of a mixture of the individual Co(OH)<sub>2</sub> and Ni(OH)<sub>2</sub> species. The same behaviour has been also observed for other bimetallic hydroxides of nickel as FeNi[39] or MnNi[29]. Therefore, the main oxidation/reduction peaks can be assigned to the oxidation of the mixed hydroxides to MO(OH) species and the corresponding reduction. However, the stationary profiles of the originally fcc or hcp deposits present some differences:

-The profiles obtained from the oxidized CoNi films with fcc phase (Co<sub>5</sub>Ni<sub>5</sub>-fcc and Co<sub>7</sub>Ni<sub>3</sub>-fcc) are more similar than that obtained from the Ni-fcc oxidized films. Moreover, a reduction shoulder at around 300mV is detected in these cases, independently of the cobalt content, shoulder that appears after or before the main reduction peak. According to the results of the Ni-fcc oxidized deposits, this cathodic peak corresponds to the reduction of NiO(OH) to α-Ni(OH)<sub>2</sub>, fact that explains the independence of its position with the Co content. Therefore, the CoNi-Ox species formed from the Co<sub>5</sub>Ni<sub>5</sub>-fcc and Co<sub>7</sub>Ni<sub>3</sub>-fcc films can be, initially, mixed hydroxides of Ni(II) and Co(II), which can be electro-oxidized to mixed MO(OH)

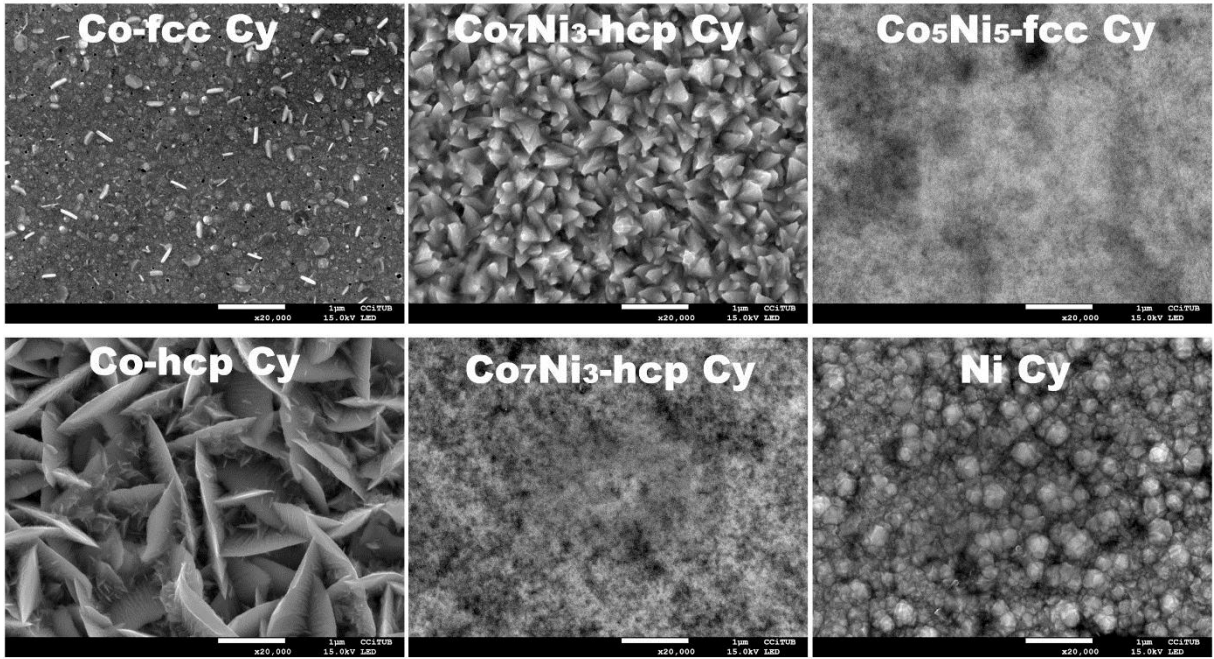
species, containing a small amount of pure Ni(III) oxo-hydroxides (NiO(OH)), next to the mixed MO(OH), which reduces to  $\alpha$ -Ni(OH)<sub>2</sub>.

-The profiles obtained from the oxidized CoNi films with high cobalt content and hcp phase (Co<sub>7</sub>Ni<sub>3</sub>-hcp) are more similar to the observed for the oxidized Co-hcp deposit. Drastic oxidation and passivation takes place during the first scan, according to the formation of metal oxides type-Co<sub>3</sub>O<sub>4</sub>, although the formation of some MO(OH) is now possible, reflected for the redox couple at 214/170 mV.

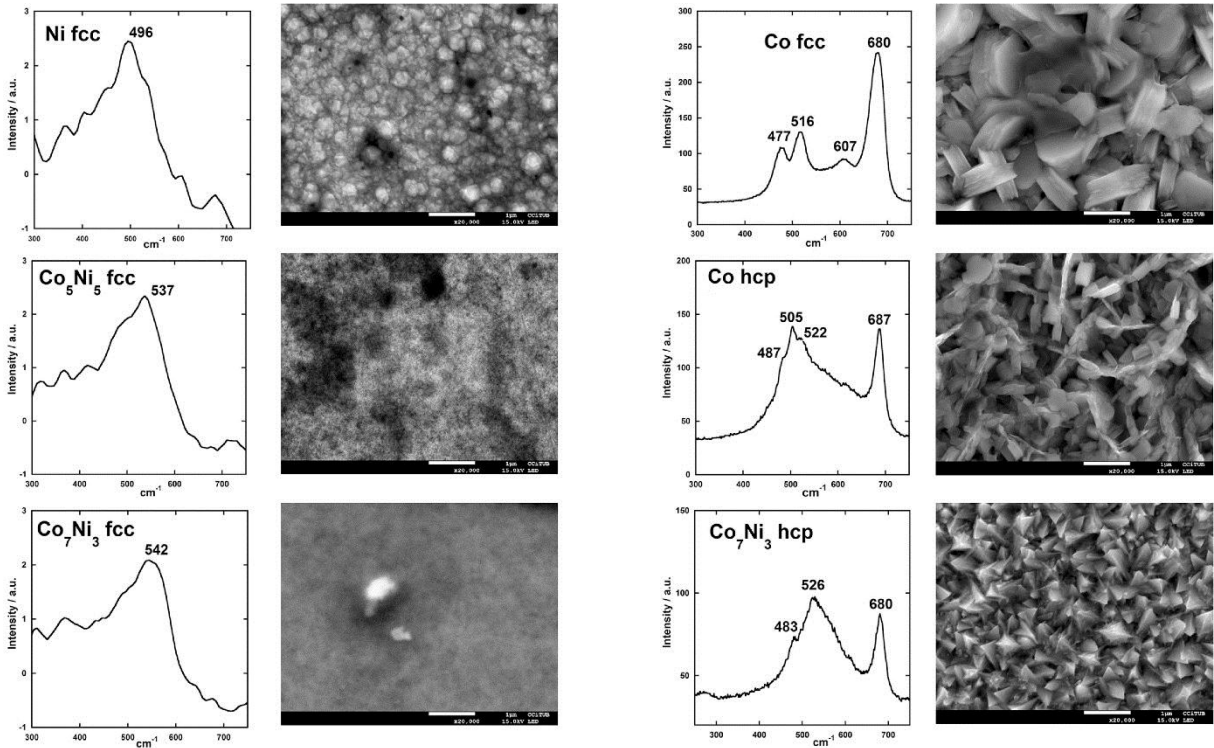
Therefore, although the cobalt content in the deposits can be high, when the electrodeposits present fcc phase, the behaviour of the oxidized films is similar to the detected for the oxidized Ni-fcc

Figure 4 shows the SEM images of each deposit after the immersion in the NaOH solution and the posterior voltammetric cycling, according to the voltammetries of the Figure 3. The comparison of these images with those obtained before the voltammetric treatment (Figure 1) allows detecting the changes produced in the surface. The Co deposits (Co-fcc and Co-hcp) maintains their original morphology, although the surface present now new crystals, probably of Co<sub>3</sub>O<sub>4</sub> oxides. The films of fcc phase (Ni-fcc, Co<sub>5</sub>Ni<sub>5</sub>-fcc, Co<sub>7</sub>Ni<sub>3</sub>-fcc) show low superficial modification and the Co<sub>7</sub>Ni<sub>3</sub>-hcp film shows an evolution of its morphology during the cycling. However, in these cases, a clear layer of oxidized species is not detected.

New replicas of each type of electrodeposit were immersed in 0.5M NaOH for 5 hours at 22°C to induce significant oxidation; after that, the oxidized layer formed in each case was observed by SEM and posteriorly analysed by means Raman Microscopy. The results are shown in the Figure 5.



**Figure 4:** SEM images of the oxidised surfaces after the voltammetric scans of Figure 3. Scale bar: 1  $\mu\text{m}$



**Figure 5.** SEM images of the oxidised surfaces after immersion of the deposits in NaOH 0.5 M during 5 hours (Scale bar: 1  $\mu\text{m}$ ) and the corresponding Raman spectra in the 300-700  $\text{cm}^{-1}$  region

The surface of the two types of Co deposits (Co-fcc and Co-hcp) shows a significant amount of oxidized species instead of the original morphology. Big crystals are observed, of similar shape than those detected after the cycling of the deposit in NaOH. The Raman spectrum shows the characteristics bands of the  $3F_{2g}$  (477 and 516  $\text{cm}^{-1}$ ),  $E_g$  (607  $\text{cm}^{-1}$ ) and  $A_{1g}$  (680  $\text{cm}^{-1}$ ) of the  $\text{Co}_3\text{O}_4$  spinel [40][R7][41][42][33][43][17]. This strong absorption at 680  $\text{cm}^{-1}$ , assigned at the highly symmetrical mode  $A_{1g}$ , is attributed to the octahedral coordination of Co(III)-O [42] in the spinel. Therefore, the  $\text{Co}_3\text{O}_4$  is the oxidized species formed from the Co-fcc deposit, both by immersion during long time and for electro-oxidation in the same basic medium. This oxide blocks the deposit, passivating its surface.

The image corresponding to the Co-hcp deposit shows also crystalline oxidised species on the surface of the deposits, but with different amount and morphology than in the case of the Co-fcc. In the corresponding Raman spectrum, the band at 687 of the  $A_{1g}$  mode of  $\text{OHC}(\text{III})\text{-O}$ , appears, but the other vibrational modes seem to be hidden by the wide band at 505  $\text{cm}^{-1}$ . As the laser power can modify the surface structure [41] and, in order to minimize this influence, the spectrum was recorded applying both the same power that in the other samples and at a power reduced until a 25% (the Raman spectrum that is shown in Figure 5 for the Co-hcp oxidized sample), remaining unchanged[41]. Therefore, the differences observed in the spectrum respect to that of the Co-fcc deposit is not due to the experimental conditions of analysis but to the presence of a new oxidized species. The wide band at 505  $\text{cm}^{-1}$  is assigned to the presence of crystalline  $\beta\text{-Co}(\text{OH})_2$ [A15] in a mixed crystalline structure of:  $\beta\text{-Co}(\text{OH})_2 + \text{Co}_3\text{O}_4$  spinel. The co-spinel structure is rejected because the no presence of the band at  $\approx 470 \text{ cm}^{-1}$ [43]. The differences in the oxidized species formed over Co-fcc( $\text{Co}_3\text{O}_4$ ) and Co-hcp ( $\text{Co}_3\text{O}_4 + \beta\text{-Co}(\text{OH})_2$ ) deposits justify also their different voltammetric behaviour. In the same way, the spectrum of the oxidised surface of the  $\text{Co}_7\text{Ni}_3\text{-hcp}$  deposit is assigned to the presence of a mixed spinel ( $\text{Co}_2\text{NiO}_4$ ) and  $a\text{Co}_x\text{Ni}_{(1-x)}(\text{OH})_2$  mixed hydroxide structure.

The SEM images of the oxidised surfaces of the deposits of cubic phase (Ni-fcc,  $\text{Co}_5\text{Ni}_5\text{-fcc}$  and  $\text{Co}_7\text{Ni}_3\text{-fcc}$ ) in Figure 5 are almost identical to those of Figure 4. Therefore, both by the cycling treatment and after immersion during long time in the basic medium, the amount of

oxides formed is low. This agrees with the very low intensity of the Raman bands in the spectra of these three deposits. According to the Raman spectra and the voltammetry experiments, the oxidized surfaces of the deposits of cubic phase contain a thin layer of crystalline  $\beta$ -Co<sub>x</sub>Ni<sub>(1-x)</sub>(OH)<sub>2</sub> with a very thin layer of the low crystalline phase  $\alpha$ -Ni(OH)<sub>2</sub> (out of Raman sensitivity).

The corrosion behaviour of the electrodeposited films has been also analysed in the NaOH 0.5 M selected medium. Figure 6 shows the typical potentiodynamic curves (in logarithmic form) to determine the values of the corrosion potential ( $E_{\text{corr}}$ ) for each deposit in the basic medium.

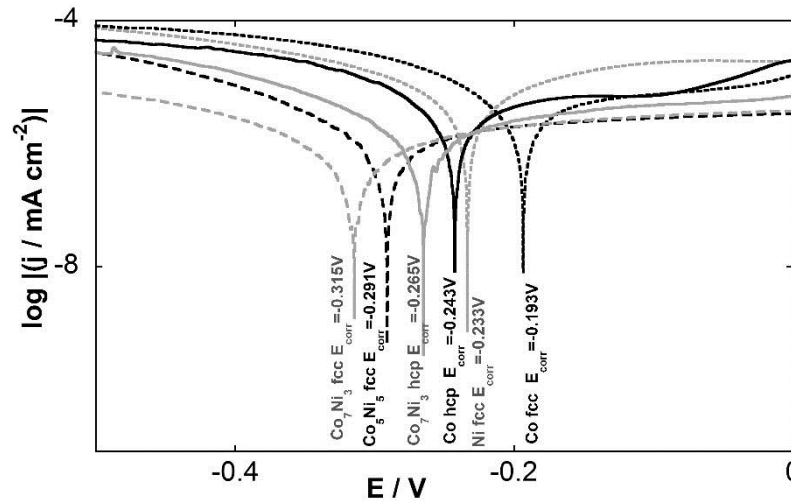


**Figure 6:** Potentiodynamic curves in NaOH 0.5M, at 0.1 mVs<sup>-1</sup>, for the different electrodeposited films.  $E$  vs Ag/AgCl/KCl 3M reference electrode.

The values obtained of the  $E_{\text{corr}}$  in basic medium for the different deposits obtained are dependent of the nobility of the metals, their crystalline phase and the passivating layers formed. Although Ni is a nobler metal than Co, the Co-fcc deposit presents higher corrosion potential due to the formation of the blocking Co<sub>3</sub>O<sub>4</sub> layer that passivates the film. When the blocking of the surface is not complete, Ni presents higher  $E_{\text{corr}}$  than Co. The Co-hcp films, according to the assigned co-structure of Co<sub>3</sub>O<sub>4</sub>+ $\beta$ -Co(OH)<sub>2</sub>, less passivating than the pure Co<sub>3</sub>O<sub>4</sub> one, present a lower value of the  $E_{\text{corr}}$  than the Co-fcc.

Mixed deposits show higher corrosion tendency than pure-metallic deposits, being this tendency, for the deposits of cubic phase, gradually increased as the cobalt percentage increases. However, the Co<sub>7</sub>Ni<sub>3</sub>-hcp presents higher  $E_{\text{corr}}$  than Co<sub>7</sub>Ni<sub>3</sub>-fcc due to the presence of the blocking spinel oxides on the surface (Co<sub>2</sub>NiO<sub>3</sub>), next to the  $\beta$ -Co<sub>x</sub>Ni<sub>(1-x)</sub>(OH)<sub>2</sub>, species.

### 3.3. Effective area of the $\text{Co}_7\text{Ni}_3\text{-fcc}$ and $\text{Co}_7\text{Ni}_3\text{-hcp}$ electrodeposits

To study the influence of the CoNi films of the same composition but different crystalline phase, by forming the M(III) oxidized species on the surface, on the urea electro-oxidation the real area of the deposits must be compared, in order to compensate the possible differences in the effective area of the electro-catalysts. As it has been shown in Figures 2,4 and 5, the morphology of the  $\text{Co}_7\text{Ni}_3\text{-fcc}$  and  $\text{Co}_7\text{Ni}_3\text{-hcp}$  deposits is clearly different, either before as after oxidation. Therefore, we try to minimize their influence in the posterior urea electro-oxidation, through the area's correction, from the surface texture parameters, measured with a confocal microscope. In the Table 2 we present some of the more significant surface texture parameters obtained from the deposits analysed in Figure 7: Sa (3D amplitude parameter equivalent to the Ra of a 2D profile) and Sq (3D amplitude parameter equivalent to the Rq of a 2D profile). As it can be seen, the amplitude parameters commonly used to evaluate the surface roughness (Sa and Sq) are only of a few nanometres in the case of the deposits of fcc phase.

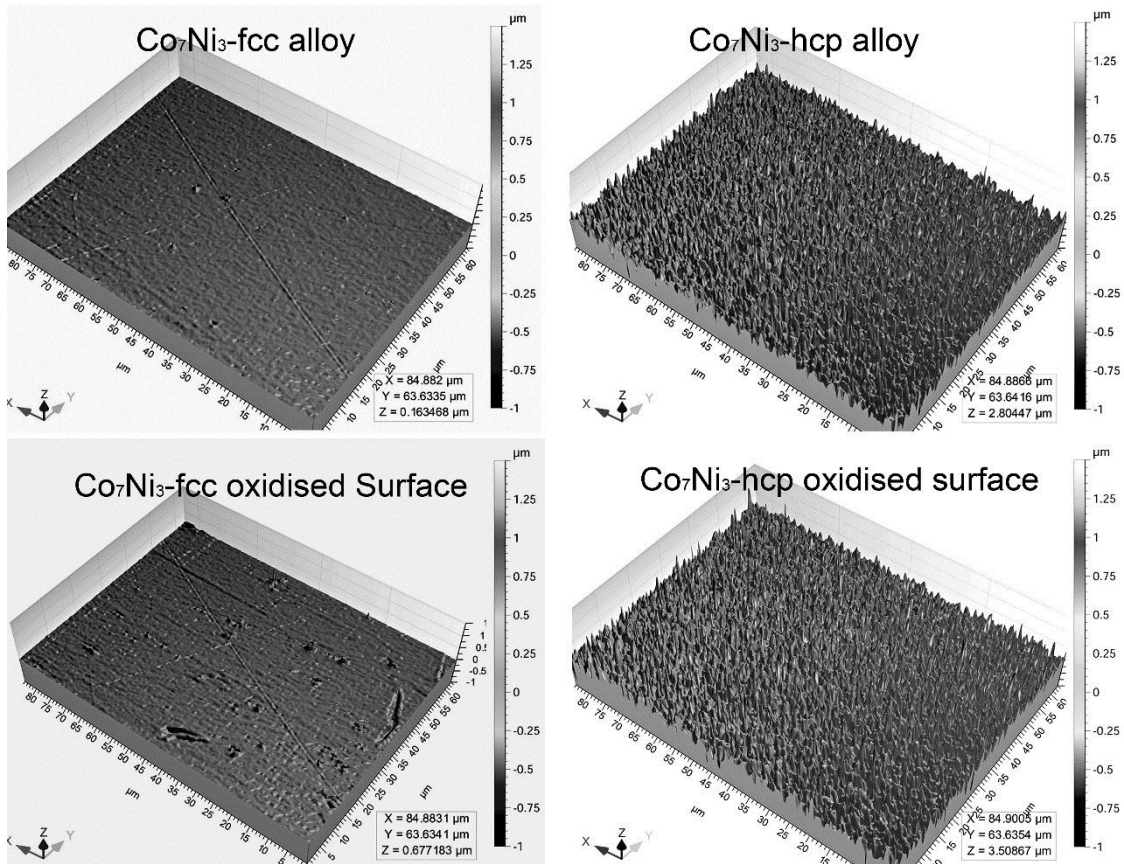


**Figure 7.** Surface texture images of the  $\text{Co}_7\text{Ni}_3$ -fcc and  $\text{Co}_7\text{Ni}_3$ -hcp electrodeposited films before and after surface oxidation

Surface Texture Parameters	$\text{Co}_7\text{Ni}_3$ hcp phase		$\text{Co}_7\text{Ni}_3$ fcc phase	
	deposited	activated	deposited	Activated
Sa ( $\mu\text{m}$ )	0.106	0.112	0.0059	0.0088
Sq ( $\mu\text{m}$ )	0.139	0.152	0.0076	0.0138
Sdar ( $\mu\text{m}^2$ )	6529.4	6770.7	5402.8	5405.9
Spar ( $\mu\text{m}^2$ )	5402.3	5402.7	5401.3	5401.5
Sdar/Spar	1.209	1.253	1.000	1.001

**Table 2.** Surface texture parameters, projected area Spar and extended area .

The images shown in the figure 7 were obtained with a confocal microscope and Leica lens EPL150x/1.2. A lens of the highest magnification was used for a maximum surface texture resolution. Even the apparent large change in the morphology seen in the SEM images of figures 2, 4, 5, the surface texture parameters are not so different. The most important parameters for our application are the  $S_{\text{par}}$  and  $S_{\text{dar}}$ .  $S_{\text{par}}$  is the surface flat projected area (similar to the area of measurement) and  $S_{\text{dar}}$  gives the extended area (area of an equivalent flat surface obtained by stretching all the mountains and valleys). The  $S_{\text{dar}}/S_{\text{par}}$  ratio informs us about the significance of the observed roughness in the real area of the surface. The Co-hcp surface shows an effective area of 120% respect of the geometrical measure, while the Co-fcc has same area as the macroscopically measured, as correspond with a flat, very fine grain surface. In the case of the oxidised surfaces the Co-hcp has an increase up to 125% of the measured macroscopic area and the Co-fcc can be considered invariant.

### **3.4. Influence of the alloy composition and crystal phase of the oxidised CoNi films in urea electro-oxidation**

Oxidized nickel-cobalt species on the deposits can catalyse the urea electro-oxidation in a similar way that occurs for methanol or glucose in basic medium. To test the influence on the catalytic electro-oxidation of the urea, the different deposited films were oxidised by means of

100 consecutive voltammetric scans in NaOH 0.5M. After the surface oxidation, urea is added to the solution and, after homogenization, new voltammetric profiles were performed in the NaOH 0.5M + urea 0.1M solution. The electrocatalytic performance of the different oxidized deposits for urea electro-oxidation was analysed and interpreted.

Figure 8 show the voltammetric profiles obtained over the oxidized deposits with fcc crystalline phase. The maximum of the urea electro-oxidation appears at around 0.5 V, followed by the drastic current increase due to oxygen evolution. When the cobalt content in the deposits increases, the catalytic activity of the surfaces decreases, as it has been also detected for other authors [35]. The previous study about the nature of the superficial oxidized species formed indicates that the catalytic activity of the  $\text{Co}_x\text{Ni}_{(1-x)}(\text{OH})_2$  species increases from  $x=1$  to  $x=0$  (for  $x=0$ , only  $\text{Co}_3\text{O}_4$ , non-active, is formed) as it was described by Yan et al. [21]. Anyway, although the higher oxidation peak is the obtained using an oxidized nickel surface, the oxidation peak slightly advances when cobalt is incorporated to the deposits.

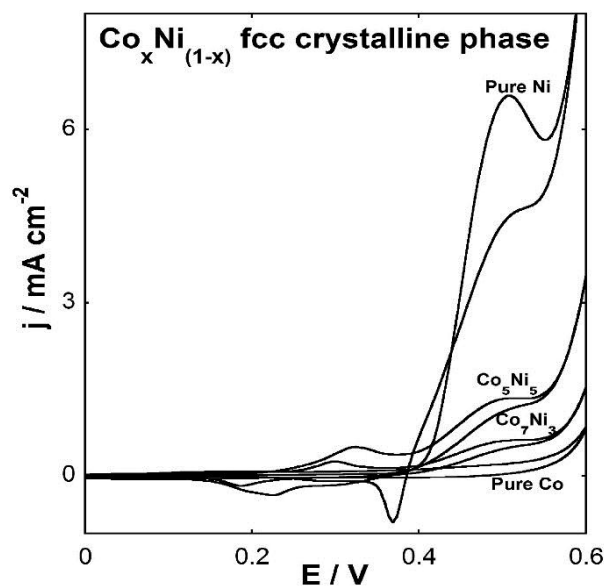


**Figure 8:** Cyclic voltammeteries at  $50 \text{ mV s}^{-1}$  in NaOH 0.5 M + 0.1 M urea solution of the different oxidized deposits with fcc crystalline phase.

Figure 9 allows us to compare the effect of the crystalline phase of the  $\text{Co}_7\text{Ni}_3$  deposits in the posterior superficial oxidation process and the catalytic behaviour respect to the urea electro-oxidation. According to the identification of the oxidized species forming during the

voltammetric cycling, we expect a difference in performance. In order to eliminate the effect of the higher roughness of the  $\text{Co}_7\text{Ni}_3$ -hcpfilm, the normalized curve according to the  $S_{\text{dar}}/S_{\text{par}}$  ratio is also included: the geometrical area was corrected by the factor of 1.25 corresponding at the  $S_{\text{dar}}/S_{\text{par}}$  value. With this correction, the effective areas for both alloys can be considered equal. Therefore, as the deposits of the same composition but different crystalline phase oxidized in a different way, they favour in different form the urea electro-oxidation. More intense and advanced oxidation peaks were observed for the  $\text{Co}_7\text{Ni}_3$ -hcpfilm and, therefore, urea oxidation is both advanced and enhanced. This study demonstrates that really cobalt-nickel alloys advance the electro-oxidation of compounds as the urea in this case, as the manner that lower potentials are necessary to induce the process. Also, the effect of the  $\text{Co}_7\text{Ni}_3$ -hcpfilms is not only due to the higher effective surface respect to the  $\text{Co}_7\text{Ni}_3$ -fcc films, but also to the influence of the crystalline phase of the deposits in the superficial oxidation process. The amount of active oxidized species of  $\text{Co}_x\text{Ni}_{(1-x)}(\text{OH})_2$  formed is higher in the case of the  $\text{Co}_7\text{Ni}_3$ -hcpfilm

The surfaces that has oxides in its composition seem to be more electrochemically actives than the composed by hydroxides as it was found for methanol oxidation by Sun et al.[35].

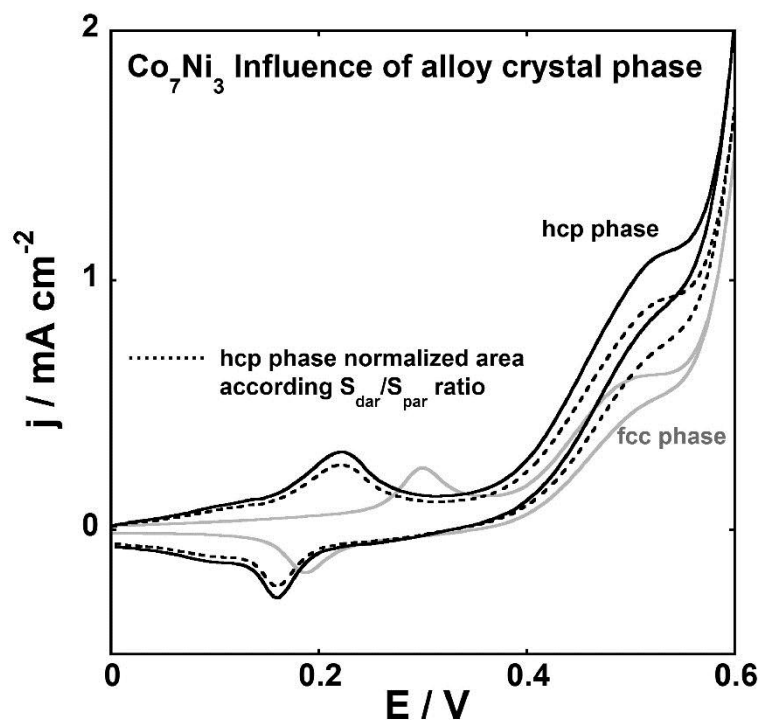


**Figure 9.** Cyclic voltammograms in NaOH 0.5 M + 0.1 M urea solution, at 50 mV s<sup>-1</sup>, of the oxidized Co<sub>7</sub>Ni<sub>3</sub> deposits. Black line: Co<sub>7</sub>Ni<sub>3</sub>-hcp and grey line: Co<sub>7</sub>Ni<sub>3</sub>-fcc deposits.

#### 4. Conclusions

The (electrodeposition + surface electro-oxidation) method has been revealed able to obtain CoNi oxidized electrodes as catalysers for urea electro-oxidation in alkaline medium. The electrodeposition has permitted the preparation of Co<sub>x</sub>Ni<sub>(1-x)</sub> films of the same composition but different crystalline structure. After voltammetric activation in alkaline medium, the oxidized layer formed is different depending on the crystalline phase of the as-deposited CoNi film. The electrodes prepared from CoNi-fcc films have superficial Ni(OH)<sub>2</sub> hydroxides, while those prepared from Co<sub>7</sub>Ni<sub>3</sub>-hcp films present a highly crystalline Co<sub>2</sub>NiO<sub>4</sub> oxide (mixed spinel) next to the Ni(OH)<sub>2</sub>. Because the catalytic species for compounds oxidation as urea are the different oxidized species formed from the fcc or the hcp deposits, the catalytic effect of the electrodes on urea electro-oxidation depends on the crystalline structure of the as-deposited CoNi films. The presence of Co in the deposited CoNi films decreases the current of urea oxidation, although it advances the potential for the electro-oxidation, which is an advantage in the urea's electrolysis for hydrogen production. The performance of oxidized Co<sub>7</sub>Ni<sub>3</sub>-hcp films for urea electro-oxidation is good, with a higher anodic current than that of the oxidized film-fcc, the lowest potential for the electro-oxidation and the lowest oxygen evolution of all the CoNi films. The electrode prepared from Co<sub>7</sub>Ni<sub>3</sub>-hcp alloy becomes a good material as anode for urea electro-oxidation.

#### Acknowledgements

This work has been supported by contract CQT2010-20726 from MINECO (Spanish Economy and Competitiveness Ministry). The authors wish to thank the Centres Científics i Tecnològics de la Universitat de Barcelona (CCiT-UB) for the use of their equipment and the IMB-CNM-CSIC (Centro Nacional de Microelectrónica) for the preparation of the substrates used.

## References:

- [1] Y.E. Roginskaya, O.V. Morozova, E.N. Lubnin, Y.E. Ulitina, G.V. Lopukhova, S. Trasatti, Characterization of bulk and surface composition of  $\text{Co}_x\text{Ni}_{1-x}\text{O}$  mixed oxides for electrocatalysis, *Langmuir* 13 (1997) 4621–4627.
- [2] M.S. Kim, T.S. Hwang, K.B. Kim, A study of the electrochemical redox behaviour of electrochemically precipitated nickel hydroxides using electrochemical quartz crystal microbalance, *J. Electrochem. Soc.* 144 (1997) 1537–1543.
- [3] M.S. Kim, K.B. Kim, A study on the phase transformation of electrochemically precipitated nickel hydroxides using an electrochemical quartz crystal microbalance, *J. Electrochem. Soc.* 145 (1998) 507–511.
- [4] A. Audemer, A. Delahaye, R. Farhi, N. Sac-Epee, J.M. Tarascon, Electrochemical and Raman studies of beta-type nickel hydroxides  $\text{Ni}_{1-x}\text{Co}_x(\text{OH})_2$  electrodematerials, *J. Electrochem. Soc.* 144 (1997) 2614–2620.
- [5] F. Wolfart, A.L. Lorenzen, N. Nagata, M. Vidotti, Nickel/cobalt alloys modified electrodes: synthesis, characterization and optimization of the electrocatalytic response, *Sens. Actuators B* 186 (2013) 528–535.
- [6] M.A. Kiani, M.A. Tehrani, H. Sayahi, Reusable and robust high sensitive on-enzymatic glucose sensor based on  $\text{Ni}(\text{OH})_2$  nanoparticles, *Anal. Chim. Acta* 839 (2014) 26–33.
- [7] B. Singh, F. Laffir, C. Dickinson, T. McCorma, E. Dempsey, Carbon supported cobalt and nickel based nanomaterials for direct uric acid determination, *Electroanalysis* 23 (2011) 79–89.
- [8] X. Tarrús, M. Montiel, E. Vallés, E. Gómez, Electrocatalytic oxidation of methanol on  $\text{CoNi}$  electrodeposited materials, *Int. J. Hydrogen Energy* 39(2014) 6705–6713.
- [9] S. Baranton, C. Coutanceau, Nickel cobalt hydroxide nanoflakes as catalysts for the hydrogen evolution reaction, *Appl. Catal. B: Environ.* 136–137 (2013) 1–8.
- [10] R. Ding, L. Qi, M. Jia, H. Wang, Facile synthesis of mesoporous spinel  $\text{NiCo}_2\text{O}_4$  nanostructures as highly efficient electrocatalysts for urea electro-oxidation, *Nanoscale* 6 (2014) 1369–1376.
- [11] H. Chen, L. Hu, M. Chen, Y. Yan, L. Wu, Nickel–cobalt layered double hydroxide nanosheets for high-performance supercapacitor electrode materials, *Adv. Funct. Mater.* 24 (2014) 934–942.
- [12] Z. Fan, J. Chen, K. Cui, F. Sun, Y. Xu, Y. Kuang, Preparation and capacitive properties of cobalt–nickel oxides/carbon nanotube composites, *Electrochim. Acta* 52 (2007) 2959–2965.
- [13] R.P. Silva, S. Eugénio, R. Duarte, T.M. Silva, M.J. Carmezim, M.F. Montemor, Electrochemical response of 70Co–30Ni highly branched 3d-dendritic structures for charge storage electrodes, *Electrochim. Acta* 167 (2015) 13–19.
- [14] V. Gupta, S. Gupta, N. Miura, Potentiostatically deposited nanostructured  $\text{Co}_x\text{Ni}_{1-x}$  layered double hydroxides as electrode materials for redox-supercapacitors, *J. Power Sources* 175 (2008) 680–685.
- [15] G. Wang, L. Zhang, J. Kim, J. Zhang, Nickel and cobalt oxide composite as a possible electrode material for electrochemical supercapacitors, *J. Power Sources* 217 (2012) 554–561.

- [16] J.P. Cheng, L. Liu, J. Zhang, F. Liu, X.B. Zhang, Influences of anion exchange and phase transformation on the supercapacitive properties of  $\gamma$ -Co(OH)<sub>2</sub>, *J. Electroanal. Chem.* 722–723 (2014) 23–31.
- [17] A.D. Jagadale, V.S. Kumbhar, R.N. Bulakhe, C.D. Lokhande, Influence of electrodeposition modes on the supercapacitive performance of Co<sub>3</sub>O<sub>4</sub> electrodes, *Energy* 64 (2014) 234–241.
- [18] H.B. Li, M.H. Yu, X.H. Lu, P. Liu, Y. Liang, J. Xiao, Y.X. Tong, G.W. Yang, Amorphous cobalt hydroxide with superior pseudocapacitive performance, *ACS Appl. Mater. Interfaces* 6 (2014) 745–749.
- [19] D. Wang, W. Yan, G.G. Botte, Exfoliated nickel hydroxide nanosheets for urea electrolysis, *Electrochem. Commun.* 13 (2011) 1135–1138.
- [20] M. Vidotti, M.R. Silva, R.P. Salvador, S.I. Cordoba, L.H. Dall’Antonia, Electrocatalytic oxidation of urea by nanostructured nickel/cobalt hydroxide electrodes, *Electrochim. Acta* 53 (2008) 4030–4034.
- [21] W. Yan, D. Wang, G.G. Botte, Nickel and cobalt bimetallic hydroxide catalysts for urea electro-oxidation, *Electrochim. Acta* 61 (2012) 25–30.
- [22] V. Vedharathinam, G.G. Botte, Understanding the electro-catalytic oxidation mechanism of urea on nickel electrodes in alkaline medium, *Electrochim. Acta* 81 (2012) 292–300.
- [23] R.L. King, G.G. Botte, Investigation of multi-metal catalysts for stable hydrogen production via urea electrolysis, *J. Power Sources* 196 (2011) 9579–9584.
- [24] S. Sun, Z.J. Xu, Composition dependence of methanol oxidation activity in nickel–cobalt hydroxides and oxides: an optimization toward highly active electrodes, *Electrochim. Acta* 165 (2015) 56–66.
- [25] J. Vilana, E. Gómez, E. Vallés, Electrochemical control of composition and crystalline structure of CoNi nanowires and films prepared potentiostatically from a single bath, *J. Electroanal. Chem.* 703 (2013) 88–96.
- [26] E. Gómez, E. Vallés, Thick cobalt coatings obtained by electrodeposition, *J. Appl. Electrochem.* 32 (2002) 693–700.
- [27] J. Vilana, D. Escalera, E. Gómez, E. Vallés, Electrochemical synthesis of Co<sub>7</sub>Ni<sub>3</sub> and Co<sub>6</sub>Ni<sub>4</sub> nanorods with controlled crystalline phase. Application to methanol electrooxidation, *J. Alloys Compd.* 646 (2015) 669–674.
- [28] V.M. Prida, J. Garcia, L. Iglesias, V. Vega, D. Görlitz, K. Nielsch, E. Díaz, R. Mendoza, A. Ponce, C. Luna, Electroplating and magnetostructural characterization of multisegmented Co<sub>54</sub>Ni<sub>46</sub>/Co<sub>85</sub>Ni<sub>15</sub> nanowires from single electrochemical bath in anodic alumina templates, *Nanoscale Res. Lett.* 8(2013) 263, 7 pp.
- [29] D.S. Hall, D.J. Lockwood, C. Bock, B.R. MacDougall, Nickel hydroxides and related materials: a review of their structures, synthesis and properties, *Proc. R. Soc. A* 471 (2014) 20140792, 65 pp.
- [30] J. Yang, H. Liu, W.N. Martens, R.L. Frost, Synthesis and characterization of cobalt hydroxide, cobalt oxyhydroxide, and cobalt oxide nanodiscs, *J. Phys. Chem. C* 114 (2010) 111–119.
- [31] Y. Du, K.M. Ok, D. O’Hare, A kinetic study of the phase conversion of layered cobalt hydroxides, *J. Mater. Chem.* 18 (2008) 4450–4459.

- [32] C. Bulet, Y. Vanbrabant, H. Goethals, T. Thys, L. Dupin, Raman spectroscopy as a tool to characterize heterogenite (CoO•OH) (Katanga Province, Democratic Republic of Congo), *Spectrochim. Acta A* 80 (2011) 138–147.
- [33] W. Yan, D. Wang, G.G. Botte, Electrochemical decomposition of urea with Ni-based catalysts, *Appl. Catal. B: Environ.* 127 (2012) 221–226.
- [34] W. Xu, H. Zhang, G. Li, Z. Wu, Nickel–cobalt bimetallic anode catalysts for direct urea fuel cell, *Sci. Rep.* 4 (2014) 5863, 6 pp.
- [35] V. Vedharathinam, G.G. Botte, Direct evidence of the mechanism for the electro-oxidation of urea on Ni(OH)<sub>2</sub> catalyst in alkaline medium, *Electrochim. Acta* 108 (2013) 660–665.
- [36] W. Yan, D. Wang, G.G. Botte, Template-assisted synthesis of Ni–Co bimetallic nanowires for urea electrocatalytic oxidation, *J. Appl. Electrochem.* 45 (2015) 1217–1222.
- [37] J.J. Huang, W.S. Hwang, Y.C. Weng, T.C. Chou, Transformation characterization of Ni(OH)<sub>2</sub>/NiOOH in Ni–Pt films using an electrochemical quartz crystal microbalance for ethanol sensors, *Mater. Trans.* 51 (2010) 2294–2303.
- [38] Y. Oaki, S. Kajiyama, T. Nishimura, T. Kato, Selective synthesis and thin-film formation of  $\gamma$ -cobalt hydroxide through an approach inspired by biomineralization, *J. Mater. Chem.* 18 (2008) 4140–4142.
- [39] L.M. Alrehaily, J.M. Joseph, M.C. Biesinger, D.A. Guzonasc, J.C. Wren, Gamma-radiolysis-assisted cobalt oxide nanoparticle formation, *Phys. Chem. Chem. Phys.* 15 (2013) 1014–1024.
- [40] Z.A. Hu, Y.L. Xie, Y.X. Wang, H.Y. Wu, Y.Y. Yang, Z.Y. Zhang, Synthesis and electrochemical characterization of mesoporous Co<sub>x</sub>Ni<sub>1-x</sub> layered double hydroxides as electrode materials for supercapacitors, *Electrochim. Acta* 54(2009) 2737–2741.
- [41] G. Hu, C. Tang, C. Li, H. Li, Y. Wang, H. Gong, The sol–gel-derived nickel–cobalt oxides with high supercapacitor performances, *J. Electrochem. Soc.* 158(2011) A695–A699.
- [42] M.G. Kast, L. Trotochaud, A.M. Smith, S.W. Boettcher, M.S. Burke, Cobalt-iron(oxy) hydroxide oxygen evolution electrocatalysts: the role of structure and composition on activity, stability and mechanism, *J. Am. Chem. Soc.* 137(2015) 3638–3648.
- [43] C.F. Windisch, K.F. Ferris, G.J. Exarhos, Synthesis and characterization of transparent conducting oxide cobalt–nickel spinel films, *J. Vac. Sci. Technol. A* 19 (2001) 1647–1651.
- [44] M.N. Iliev, P. Silwal, B. Loukya, R. Datta, D.H. Kim, N.D. Todorov, N. Pachauri, A. Gupta, Raman studies of cation distribution and thermal stability of epitaxial spinel NiCo<sub>2</sub>O<sub>4</sub> films, *J. Appl. Phys.* 114 (2013) 033514, 5 pp.
- [45] C.F. Windisch, G.J. Exarhos, R.R. Owings, Vibrational spectroscopic study of the site occupancy distribution of cations in nickel cobalt oxides, *J. Appl. Phys.* 95 (2004) 5435–5442.
- [46] C.F. Windisch, G.J. Exarhos, S.K. Sharma, Influence of temperature and electronic disorder on the Raman spectra of nickel cobalt oxides, *J. Appl. Phys.* 92 (2002) 5572–5574.
- [47] R. Deltombe, K.J. Kubiak, M. Bigerelle, How to select the most relevant 3D roughness parameters of a surface, *Scanning* 36 (2011) 150–160.